FULL PAPER

Steady-state and time-resolved optical properties of multilayer film of titanium dioxide sandwiched by gold nanoparticles and gold thin film

Shin-ichiro Yanagiya*[a], Toshihiko Takahata[a], Yuki Yoshitani[a], Retsuo Kawakami[a], and Akihiro Furube[a]

Dedication ((optional))

Abstract: We proposed metal-insulator (MI) and metal-insulator-metal (MIM) structures of titanium dioxide (TiO_2) sandwiched by gold nanoparticles (AuNPs) layer and gold sputtered thin film (only for the MIM film) to couple localized plasmon mode of AuNP with multi-reflection mode and/or cavity resonator mode of TiO_2. The optical extinctions of MI and MIM with differing TiO_2 thickness were studied theoretically by finite-element method simulation and experimentally by optical spectrometry. The extinction peaks of MI and MIM shifted by exchanging the surrounding medium from air to TiO_2. The interference of TiO_2 in MI structure also affected the extinction spectra showing the oscillation along the spectrum of AuNP in TiO_2. Then, the extinction degree of MIM was higher than that of MI because of the coupling between cavity resonance mode with localized plasmon mode and interband transition in AuNPs. In addition, the cross section of MI and MIM films were observed by scanning electron microscopy. The surface of thinner film was rough because TiO_2 heterogeneously grew from AuNP. The irregular growth of TiO_2 might have induced the wide-range extinction in 300-2500 nm after Au thin film deposition. The transient absorption spectra using a femtosecond laser were also carried out under the condition of 800 nm for excitation laser and 950 nm for probe laser. The long-lived electron (~1 ns) was observed in thick MIM film as a result of hot electron transfer from the gold nanostructure in the film.

1. Introduction

Titanium dioxide (TiO_2) is promising for applications in areas such as optics,[1] opto-electronics,[2] and photochemistry.[3,4] Especially, TiO_2 is well known as photocatalytic materials that absorb ultraviolet (UV) [3,5] and it is promising a dye-sensitized solar cell, self-cleaning exterior and cleaning wastewater applications.[2,6,7] Although TiO_2 single crystal is transparent from visible to infrared (IR) range, the powder form of TiO_2 has white color due to its scattering light and, thus, commercially available as white pigment in cosmetics, paints, papers, and inks.[8] In addition, TiO_2 film, if the film thickness is the same as the wavelength of light, shows interference colors and commercially available as an optical color filter. To utilize the sunlight effectively, it is necessary to extend the absorbance of TiO_2 from the ultra-violet (UV) region to the visible and IR regions. One of the technologies achieving this is to combine the TiO_2 with gold nanoparticles (AuNPs).

AuNPs also draw researchers' attention in the area of plasmonics.[9–15] Au in bulk form absorbs blue and green light and reflects other visible light, which results in a shining golden color. On the other hand, AuNPs strongly interact with light that originates from the excitation of collective oscillation of their surface charges named as localized surface plasmon resonance (LSPR). The excited AuNP creates hot charge carriers, which partially give their energy to the lattice for nano-heating [16–18] or transfer to neighbor materials if exceeding chemical potential barriers. TiO_2 is especially suitable as the neighbor material because of an optical absorbance band difference and its photocatalytic characterizations.

Nanocomposites of TiO_2 and Au are promising for applications in areas such as photocatalyst,[19,20] plasmonic biosensing,[21,22] and solar energy harvesting.[23–26] In earlier studies, TiO_2 nanocrystals were integrated with AuNPs, which enhanced the absorption of visible light due to its LSPR absorption.[27] Some studies focused on the development of AuNP/TiO_2 nanocomposites in powder form.[23,24] Other synthetic approach such as a sol-gel method [28] was reported for nanocomposite thin film. In addition, metal-insulator-metal (MIM) structure of Au-TiO_2-Au fabricated by dry process has been recently reported as an efficient light absorber and photocurrent generators.[21,22,29,30] In the system, the localized plasmon mode of AuNP was coupled with photonic mode of TiO_2.[20,31,32] In the study, we fabricated the AuNPs colloidal self-assembly on glass to act not only as localized plasmonic nano structure but also as optically flat semi-transparent layer. Also, the thin Au-film (<20 nm in thickness) was sputtered on MI film because of its semi-transparency without LSPR.

There are some fabrication techniques for Au nanostructures; Au thin film is grown by vapor growth such as physical deposition and sputtering method, and Au nano-particles, nano-cubes, and nano-rods are grown by solution growth named as seed mediated method.[33–35] In this study, multilayer nano-

[a] S. Yanagiya (Corresponding author, Assist. Prof.), T. Takahata (Grad. Stud.), Y. Yoshitani (Grad. Stud.), R. Kawakami (Assist. Prof.), and A. Furube (Prof.)
Graduate School of Science and Technology,
Tokushima University
2-1 Minamijosanjima-cho, Tokushima, 770-8506, Japan
E-mail: syanagiya@tokushima-u.ac.jp

structured films of TiO_2 sandwiched by AuNPs and Au thin film were prepared on a glass substrate. AuNPs were prepared by citrate reduction method and deposited onto silane treated glass substrate. Then, TiO_2 films of 130-800 nm in thickness were deposited by magnetron sputtering method. Au thin film was deposited on the TiO_2 layer by sputtering method to achieve MIM structure. Extinction spectra of the films were explored from the reflection and the transmission spectra, which were measured with an UV-visible-near infrared (UV-Vis-NIR) spectrometer. The extinction of the films was also studied with a finite-element method (FEM) simulation of wave optics. The MI and MIM structures of the films, which affect the light scattering of the film, were investigated by scanning electron microscopy (SEM). Femtosecond transient absorption spectra were also evaluated for the MIM films to characterize the behaviors of hot electrons in the film under 800 nm excitation.

2. Results and Discussion

2.1 Design and numerical results of MI and MIM structures

Main Extinction spectra of the films were first theoretically studied by FEM simulation with COMSOL multiphysics.[36] Figure 1 shows the schematic diagrams of proposed models of TiO_2-AuNP (MI) and Au thin film-TiO_2-AuNP (MIM) structure. AuNP of 40 nm in diameter was placed on a glass and covered by TiO_2. The thickness of TiO_2, *d*, was changed from 0 (AuNP surrounded by air) to 800 nm. The MI film was sandwiched by surrounding air and glass layers whose thickness were set to the same. The size of total calculation box was set to 100 × 100 × 3000 nm^3. The *x*-*y* plane had a periodic boundary condition, which indicated that the particle density of AuNPs was set to 100 units per μm^2. A monochromatic incident light ranged from 400 to 2500 nm in wavelength, I_0, was inserted from bottom with a power of 1 W/m. Reflected light (*R*, red arrow) and transmitted light (*T*, blue arrow) were calculated with frequency modulation method in a wave optics module of COMSOL. Then the optical extinction, *E*, was calculated from the relationship of $E = (I_0 - T - R)/I_0$. To propose the MIM composite film, Au thin film with a thickness of 14 nm was set at the interface between the TiO_2 and the air layers as shown in Fig.1(b). The optical properties of AuNP and Au film were subjected to Lemarchand model [37] In the previous study, TiO_2 was grown on a glass surface and characterized as bronze phase by X-ray diffraction analysis.[38] Because the bronze phase has the simlar structure with anatase and we chose the dielectric model of Kischkat in this study [39].

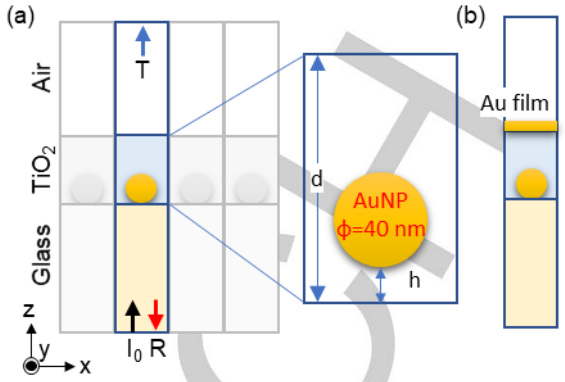

Figure 1. Schematic diagrams of (a) the MI and (b) the MIM structure models used in this study. In each model, surrounding air was taken into account. The film layer TiO_2 was located between the glass and the air. An AuNP of 40 nm in diameter in the TiO_2 layer with a thickness of *d* was set at a gap distance of *h* from the glass surface. The optical reflectance (*R*, red arrow) and transmittance (*T*, blue arrow) as a function of frequency were calculated assuming that the initial light, I_0, inserted from the bottom into the films.

For instance, transmittance (*T*), reflectance (*R*), and extinction (*E*) spectra of the MI and the MIM structure models for the TiO_2 layers of 800 nm in thickness are shown in Fig. 2. The calculated *T* and *R* oscillated with the wavelength and had a distinctive peaks in the wavelength range of 600 to 800 nm. In previous studies, it was reported that the dual mode splitting was attributed to the strong interaction between the plasmonic resonance and the cavity resonance.[20,31,32] Comparing Fig. 2(a) with 2(b), the calculated *T* and *R* of MIM were smaller than those of MI structure in the range of 400-600 nm. This is due to the absorbance Au-film and thus the calculated *E* of MIM resulted in becoming larger.

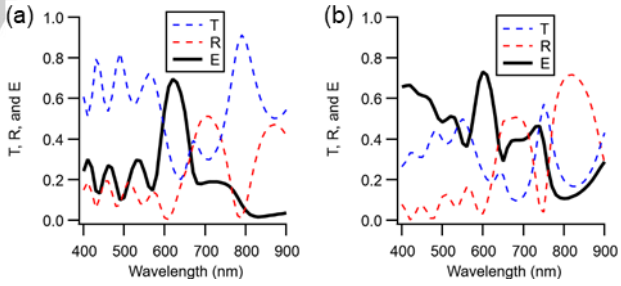

Figure 2. Simulation results of optical transmittance (*T*), reflection (*R*), and extinction (*E*) spectra of the (a) MI and (b) MIM structure models with TiO_2 film thickness of 800 nm.

To further study, the extinction curves for a variety of TiO_2 layer thickness were put together in Fig. 3. The overlapped extinction curves seemed to be coalesced into a large peak, which had a peak wavelength of about 630 nm and almost the same maximum value (~0.8) in spite of MI and MIM structures. For comparison, the calculated extinction curves of AuNP surrounded in air (red dotted curve) and in TiO_2 (black dashed curve) are also drawn in Figs. 3(a) and 3(b). The extinction curves, which were

calculated from FEM simulation, agreed well with the results of Mie scattering theory.[40–42] As shown in Fig. 3(a), the extinction curve of MI structure was oscillated along the dashed curve. This indicates that the extinction of AuNP was enhanced by exchanging its surrounding medium from air to TiO_2 and was oscillated by the multi-reflection from TiO_2 layer. The extinction at a thickness of 100 nm was smaller than the other spectra because the TiO_2 layer might be too thin to oscillate owing to multi-reflection. Compared to the spectra of MI structure models, the overlapped extinction curves of MIM was larger. As shown in Fig. 3(b), the minimum of the overlapped extinction was approximated by the curve of Au-film. This indicates that the Au-film acted more of a resonant mirror than an optical absorber. Moreover, at wavelengths more than 900 nm, the extinction remained between 0.1 and 0.3. This is caused by the interband transition of Au-film and the strong interaction between the plasmonic resonance of AuNP and the cavity resonance of TiO_2. To conclude the FEM simulation, the MI film show the coupling of the LSPR shift by changing the surrounding medium from air to TiO_2 with the multi reflection in the TiO_2 film. On the other hand, the MIM films increased their extinction in the wide region of 400-2500 nm. The absorption of Au-film was dominant in 400-600 nm, and besides, the coupling of the plasmonic resonance of AuNP with the cavity resonance might be dominant.

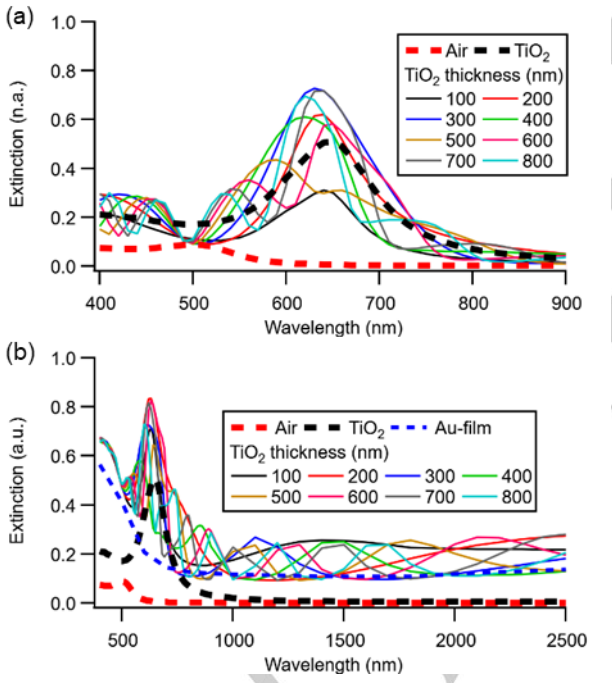

Figure 3. Calculated extinction spectra of (a) the MI and (b) the MIM structure models. For comparison, the calculated extinction spectra of AuNP in air (red dotted curve) and in TiO_2 (black dashed curve) are also drawn in the figures. Blue dotted curve in (b) is the simulated extinction of Au-film on glass excluding AuNP and TiO_2.

2.2 Experimental results and discussion

Figure 4(a) shows an optical image and optical extinction of AuNPs on a glass. The AuNPs were pink and had the extinction peak at 539 nm due to LSPR. The AuNP of 40 nm in diameter had the absorbance peak at 520 nm in a solution. This red shift was supposed to be caused by changing from solution to air and aggregating AuNPs during drying on a glass. Figure 2(b) shows optical images of the MI and MIM film. The left half of the sample was masked after sputtering TiO_2 on AuNP, and sputtered Au for fabricating the MIM films. The color of MI film was blue or purple, which changed depending on the thickness of TiO_2 layer. The MI film was so transparent that we can clearly see grids drawn on the paper through the film. On the other hand, the MIM film was so dark as to blind the grids.

Figures 4(c)-4(f) show FE-SEM images of the side view of fabricated films. In the previous study, the sputtered TiO_2 film on glass was characterized as bronze phase and changed to anatase phase after thermal treatment.[38] In the study, the film phase was considered to be bronze phase because the films were fabricated without thermal treatment. As shown in Fig. 4(c), the MI film was rough when the TiO_2 was 130 nm in thickness, though the film was flat without AuNP as shown in Fig. 4(e). The sputtered TiO_2 seemed to nucleate heterogeneously from an AuNP and grew perpendicularly to the substrate with a columnar form as shown in Fig. 4(d) and 4(f). The line density of AuNP was 1-2 units per 130 nm and then the widths of TiO_2 became thicker from 50 to 150 nm during the growth of TiO_2 from 130 nm to 400 nm. In addition, the head of the TiO_2 columnar were rounded and this induced the surface roughness of MI and MIM films.

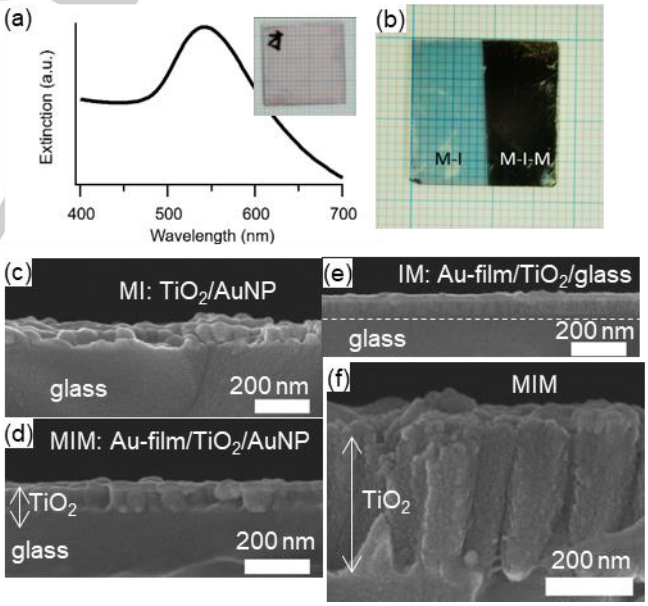

Figure 4. (a) Extinction curve of AuNP mono-layer on glass. The inset photograph is a glass covered by AuNPs. (b) Photograph of the fabricated MI and MIM films on a glass. (c-f) SEM images of (c) MI, (d) MIM, and (e) IM (w/o AuNP) films with TiO_2 thickness of 130 nm and (f) MIM film with TiO_2 thickness of 400 nm. Cross-section of the sample was obtained by cutting the glass substrate from the bottom.

Next, steady-state optical properties of MI and MIM films were investigated. Figure 5(a) and 5(b) show the reflectance and the transmittance of MI films with different TiO_2 thickness

measured by optical spectrometry. As shown in Fig. 5(a), the wavelength of transmittance edges of MI film shifted from 320 to 380 nm as the thickness of TiO_2 layer increased from 130 to 800 nm. Since the wavelength of transmittance edge were longer than that of absorbance edge of glass, the wave length shift in the transmittance edge might be due to the bandgap change of TiO_2 layer. The transmittance oscillated in the case that the TiO_2 was thicker than 400 nm. On the other hand, the reflectance oscillated in all wavelength range and the oscillation period shortened when the TiO_2 became thicker. This result indicates that the MI film showed the multi interference of TiO_2. Figure 5(c) shows the extinction The peak appearing in wavelengths of 600-800 nm described in Fig. 3 was observed in Fig. 5(c), too. However, the intensity was not as large as the simulation result. As shown in Fig. 4(c), the rough surface of MI produced a scattering light, which was responsible for the resonance in TiO_2 layer. In addition, AuNP's size distribution may be responsible for the extinction decrease.

The extinction spectra for MIM films were shown in Fig. 5(d). Compared to the MI films, the MIM film provided a higher extinction and oscillated with a larger amplitude in the visible light region. The results were identified in the computational results, which suggests that the high extinction of MIM film is due to the interband transition of AuNP and Au-film. In addition, the MIM films with the TiO_2 layer thickness of 130 and 200 nm showed a higher extinction in an infrared region, which remained more than 60% at a wavelength of 1000 nm. The simulation results in Fig. 3(b) indicated that the MIM film showed the extinction oscillated between 10-30 % at 1000-2500 nm. The reason for the difference between the experimental and computational extinction spectra was supposed to be due to the surface condition of MI and MIM films. As shown in Fig. 4(c)-4(f), The irregularity of Au-film provide the localized surface plasmon (LSP) with retrograded SPPs. This might be the reason why the unexpected near-IR (NIR) extinction was observed.

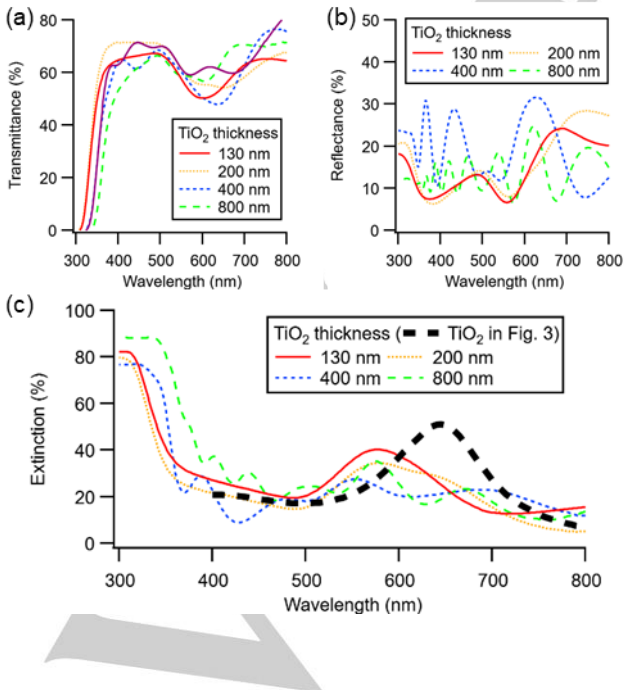

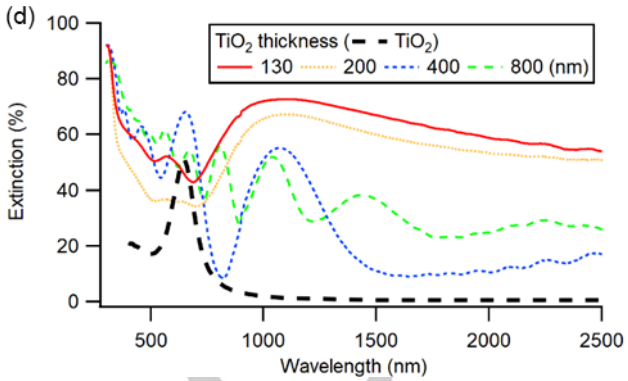

Figure 5. The spectrum curves of (a) transmittance, (b) reflectance, and (c) extinction of MI film with differing TiO_2 thicknesses. (d) The extinction spectra of MIM film. The black dashed curve was the FEM simulation result of AuNP surrounded by TiO_2, which was replotted from Fig. 3.

Finally, time-resolved spectroscopy was utilized to characterize the optical response of the MIM films under 800 nm excitation. Note that 800 nm light is hardly absorbed in all the MI films, so here we observe carrier dynamics exciting newly induced optical transitions by forming the MIM structures.

Figure 6 shows the transient absorption intensities of MIM films of different TiO_2 thickness. When the TiO_2 was relatively thin (130 nm and 200 nm in TiO_2 thickness), the absorbance signal immediately fell down and recovered mostly within 10 ps. This is supposed to be assigned to plasmon band bleaching as reported by Link et al. previously[43]. In previous transient absorption studies of AuNPs, it was reported that the signal of transient bleaching recovers owing to electron-phonon and phonon-phonon relaxation with molecules in the surrounding medium with lifetimes of the order of 1~4 and 100 ps, respectively. Since the large extinction values (> 60%) at the probe wavelength of 950 nm are obtained in a broad NIR band (see Fig. 5(d)) and the pump wavelength corresponds to a part of the same band, the decay process of the bleaching is assigned to the electron-phonon relaxation.

On the contrary, when the TiO_2 thickness increased, the contribution of bleaching is almost hidden and instead the positive signals became dominant having slow decay to the sub-nanosecond scale. The positive signals were also observed during the cooling process at the wavelength close to the LSP peak.[44] However, this lifetime is less than 100 ps, which was shorter than that measured in this study. Du *et al.* reported that the electron injection mechanism in gold-TiO_2 nanoparticle system under the condition of 550 nm in a pump laser.[45] They have observed appearance of positive IR signals assigned to the conductive electrons in TiO_2. Plasmon-induced electron transfer was within 50 fs and charge recombination (back electron transfer from TiO_2 to AuNP) was in the sub-nanosecond time scale. Similar dynamics is observed by Bian *et al.* with NIR probe [46] Therefore, we assign the positive transient absorption to electrons injected from gold in the MIM structures.

The transient absorption time profiles were fitted with two components binominal exponential model, that is;

$y = A_1 \exp\left(-\frac{x-x_0}{\tau_1}\right) + A_2 \exp\left(-\frac{x-x_0}{\tau_2}\right) + y_0$,

where $A_{\{1,2\}}$ and $\tau_{\{1,2\}}$ represent the amplitude and lifetime of electron-phonon and phonon-phonon interactions if only cooling process of gold is observed.[43] The total amplitude *y* depending on the time *x* was fitted by mean square method. The resulted curves are drawn in Fig. 6 and the parameter of τ_1 and τ_2 were summarized in Table 1. The short τ_1 (< 5 ps) was obtained in the relatively thin TiO_2 films (130 and 200 nm), while τ_2 components were not clearly recognized. Fitting procedure was applied only for decaying part after the signal maximum for thick TiO_2 films (400 and 800 nm) to analyze the lifetimes of injected electrons. Because of measured time range up to 1 ns, the estimated lifetimes longer than ~500 ps are not reliable, but surely indicates the presence of long-lived electrons in these films in addition to the component with τ_1 of 70 ps for the 800-nm thickness film. Positive electron signals and negative bleaching signals decaying in the order of 100 ps may cancel each other for the thin TiO_2 films.

For our MIM films, we suppose that the optical excitation at the wavelength of 800 nm was also found to be the LSP band of AuNPs conjugated with SPPs along the interface of TiO_2 and AuNPs. This excitation mode resulted in generation of conductive electrons in TiO_2, which can be beneficial for future applications such as solar cells, photo-detection, photocatalysis and photoelectrochemical sensing in the NIR range.

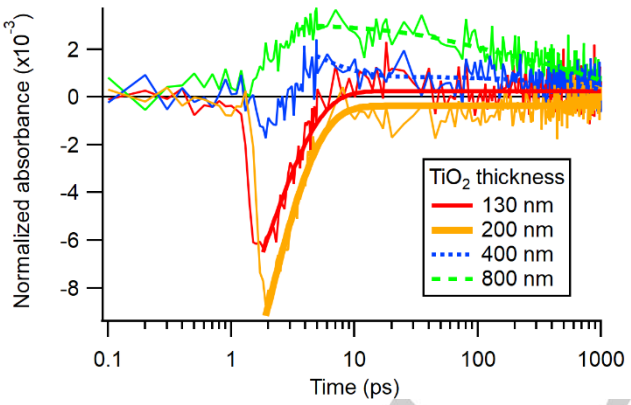

Figure 6. Transient absorption spectra of MIM films with different TiO_2 thickness.

Conclusions

The MI films were fabricated by growing TiO_2 on AuNPs-coated glass with sputtering, and the MIM films by growing Au film on the MI films with sputtering. The MI films showed blue or purple color with transparency. The extinction of MI had the peak between 600 and 800 nm and oscillated along that of AuNP in TiO_2, which was assigned the coupling of the LSPR shift by changing the surrounding medium from air to TiO_2 with the multi reflection in the TiO_2 film. On the other hand, the MIM films showed a high extinction and a high amplitude in the whole wavelength region between 300 and 2500 nm, not only 600-800 nm. The absorption of Au-film was dominant in 400-600 nm, and besides, the coupling of the plasmonic resonance of AuNP with the cavity resonance might be dominant. We concluded that the extinction spectra in this study were determined from three factors; (1) LSPR change of AuNP surroundings from air to TiO_2, (2) TiO_2 film thickness to enhance the extinction of AuNP, and (3) surface morphology of Au thin film. Femtosecond transient absorption revealed that the MIM films are capable of charge generation in the TiO_2 semiconductor part under 800 nm excitation.

Table 1. Parameters of τ_1 and τ_2 with different TiO_2 film thickness.

TiO_2 thickness	130 nm	200 nm	400 nm	800 nm
τ_1 (ps)	1.8808	1.9465	4.2165	68.664
τ_2 (ps)			1861.7	861.88

Experimental Section

AuNPs with a diameter of 40 nm were synthesized by citrate reduction in an aqueous solution. A stock solution was prepared by dissolving $HAuCl_4 \cdot 2H_2O$ (1 g, Kishida Chemicals, 99.9%) in doubly distilled water (10 mL) to render a 0.25 M $HAuCl_4$ aqueous solution. An aliquot of this solution (100 mL) was heated to boiling temperature before adding 10 mg/mL aqueous trisodium citrate (1 mL, Wako Pure Chemicals) under vigorous stirring. Afterwards, the solution was stirred for 15 min without heating and then boiled for an additional 15 min. The resulting colloidal AuNPs were assembled on cover slip surfaces (Matsunami, borosilicate glass) functionalized with 3-aminopropyltrimethoxysilane (APTMS, Wako Pure Chemicals, > 98%). Specifically, glass substrates (18 ×18 × 0.5 mm^3) were silanized in the presence of mixture of 40 mL ethanolic APTMS for 1 h at 60 ℃. The APTMS-functionalized surfaces were rinsed four times successively with ethanol and distilled water before being placed in an AuNP solution for 12 to 18 h at 10 ℃. The coated substrates were washed with distilled water and dried.

Next, TiO_2 was deposited on the substrate by direct current (DC) facing-target sputtering method. The targets were Ti metal plates (99.9 % purity). The AuNPs-coated glass substrate was set perpendicular to the plates in a vacuum bell jar. The pressure in the bell jar was once decreased below 1.53×10^{-4} Pa and increased at 1.6 Pa by flowing the mixture of Ar and O_2 gases at an Ar/O_2 gas flow ratio of 3:2. The total gas flow rate was kept constant at 4.2 sccm. The Ar/O_2 plasma was generated by two DC power supplies with a voltage of 490 ± 10 V applied to the Ti targets, respectively. The thickness of sputter-deposition film was varied by changing the deposition time while keeping the plasma-generating conditions.

Au thin film was deposited on the MI film using ion sputtering coater (Hitachi E-1010). The Au target (63 mm in diameter) was set to face the sample. The sputtering pressure in the vacuum chamber was kept at 10 Pa in Ar atmosphere. The coating time and discharge current were 250 s and 15 mA, respectively, to fabricate Au film of 15 nm thickness.

Optical properties of the films were evaluated by a UV-Vis-NIR spectrometer (JASCO V-770). Reflectance (*R*) and transmittance (*T*) spectra were measured using the accessory of specular reflectance

accessory (JASCO SLM-907) and film holder (JASCO VTA-752) with a light incident angle of 5°. The wavelength range was 300-800 nm for the MI films and 300-2500 nm for the MIM film. The optical extinction (*E*) was estimated from the relationship of $E = I_0 - T - R$, as in the case of the simulation models described above. Cross sections of MI and MIM films were investigated by scanning electron microscopy (FE-SEM, Hitachi S-4700). Cross-section of the sample was obtained by cutting the glass substrate from the bottom.

Femtosecond transient absorption spectra were also evaluated for the MIM films. Some experimental details were described previously [23]. The light source for pump and probe was a femtosecond titanium sapphire laser with a regenerative amplifier (Hurricane, Spectra Physics, 1.0 mW, 500 Hz). The pump laser of 800 nm in wavelength went through the sample after entering the decay stage to change the pulse distance to achieve a time delay. The probe beam was obtained by inducing into a white-light continuum generation device. The probe laser transmitted the sample and detected at 950 nm with optical spectrometer. Transient absorption intensity was calculated from the pulse intensity of the probe with and without excitation, typically using thousands of pulses. The sample of MIM films were placed in air during the measurements.

Acknowledgements

Acknowledgements Text.

Keywords: Titanium dioxide • Gold nanoparticle • Gold thin film • Optical extinction • Transient absorption spectroscopy

[1] Jeong, S.H., Kim, J.K., Kim, B.S., Shim, S.H., and Lee, B.T. *Vacuum*, 2004, 76 (4), 507–515.
[2] O'Regan, B., and Grätzel, M. *Nature*, 1991, 353 (6346), 737–740.
[3] Fujishima, A., Rao, T.N., and Tryk, D.A. *J. Photochem. Photobiol. C Photochem. Rev.*, 2000, 1 (1), 1–21.
[4] Hashimoto, K., Irie, H., and Fujishima, A. *Jpn. J. Appl. Phys.*, 2005, 44 (12), 8269–8285.
[5] Awazu, K., Fujimaki, M., Rockstuhl, C., Tominaga, J., Murakami, H., Ohki, Y., Yoshida, N., and Watanabe, T. *J. Am. Chem. Soc.*, 2008, 130 (5), 1676–1680.
[6] Carp, O., Huisman, C.L., and Reller, A. 2004, 32, 33–177.
[7] Nan, M., Jin, B., Chow, C.W.K., and Saint, C. *Water Res.*, 2010, 44 (10), 2997–3027.
[8] Weir, A., Westerhoff, P., Fabricius, L., Hristovski, K., and Goetz, N. Von 2012,.
[9] Baffou, G., Quidant, R., and Girard, C. *Phys. Rev. B*, 2010, 82 (16), 165424.
[10] Setoura, K., Werner, D., and Hashimoto, S. *J. Phys. Chem. C*, 2012, 116 (29), 15458–15466.
[11] Katayama, T., Setoura, K., Werner, D., Miyasaka, H., and Hashimoto, S. *Langmuir*, 2014, 30 (31), 9504–9513.
[12] Donner, J.S., Baffou, G., McCloskey, D., and Quidant, R. *ACS Nano*, 2011, 5 (7), 5457–5462.
[13] Matsumura, H., Yanagiya, S., Nagase, M., Kishikawa, H., and Goto, N. *Jpn. J. Appl. Phys.*, 2016, 55, 06GL05.
[14] Yanagiya, S., Sekimoto, N., and Furube, A. *Jpn. J. Appl. Phys.*, 2018, 57 (11), 115001.
[15] Amendola, V., Pilot, R., Frasconi, M., Maragò, O.M., and Iatì, M.A. *J. Phys. Condens. Matter*, 2017, 29 (20).
[16] Metwally, K., Mensah, S., and Baffou, G. *J. Phys. Chem. C*, 2015, 119 (51), 28586–28596.
[17] Lukianova-Hleb, E., Hu, Y., Latterini, L., Tarpani, L., Lee, S., Drezek, R.A., Hafner, J.H., and Lapotko, D.O. *ACS Nano*, 2010, 4 (4), 2109–2123.
[18] Baffou, G., and Quidant, R. *Laser Photonics Rev.*, 2013, 7 (2), 171–187.
[19] Yuzawa, H., Yoshida, T., and Yoshida, H. *Appl. Catal. B Environ.*, 2012, 115–116, 294–302.
[20] Shi, X., Ueno, K., Oshikiri, T., Sun, Q., Sasaki, K., and Misawa, H. *Nat. Nanotechnol.*, 2018, 13 (10), 953–958.
[21] Hackett, L.P., Ameen, A., Li, W., Dar, F.K., Goddard, L.L., and Liu, G.L. *ACS Sensors*, 2018, 3 (2), 290–298.
[22] Hackett, L.P., Li, W., Ameen, A., Goddard, L.L., and Liu, G.L. *J. Phys. Chem. C*, 2018, 122 (11), 6255–6266.
[23] Furube, A., Du, L., Hara, K., Katoh, R., and Tachiya, M. *J. Am. Chem. Soc.*, 2007, 129 (48), 14852–14853.
[24] Tian, Y., and Tatsuma, T. *J. Am. Chem. Soc.*, 2005, 127 (20), 7632–7637.
[25] Brongersma, M.L., Halas, N.J., and Nordlander, P. *Nat. Nanotechnol.*, 2015, 10 (1), 25–34.
[26] Nishijima, Y., Ueno, K., Yokota, Y., Murakoshi, K., and Misawa, H. *J. Phys. Chem. Lett.*, 2010, 1 (13), 2031–2036.
[27] Dahl, M., Liu, Y., and Yin, Y. *Chem. Rev.*, 2014, 114 (19), 9853–9889.
[28] Buso, D., Pacifico, J., Martucci, A., and Mulvaney, P. *Adv. Funct. Mater.*, 2007, 17 (3), 347–354.
[29] Ng, C., Cadusch, J.J., Dligatch, S., Roberts, A., Davis, T.J., Mulvaney, P., and Gómez, D.E. *ACS Nano*, 2016, 10 (4), 4704–4711.
[30] Fang, Y., Jiao, Y., Xiong, K., Ogier, R., Yang, Z.J., Gao, S., Dahlin, A.B., and Käll, M. *Nano Lett.*, 2015, 15 (6), 4059–4065.
[31] Christ, A., Tikhodeev, S.G., Gippius, N.A., Kuhl, J., and Giessen, H. *Phys. Rev. Lett.*, 2003, 91 (18), 1–4.
[32] Ameling, R., and Giessen, H. *Nano Lett.*, 2010, 10 (11), 4394–4398.
[33] Niu, W., Zhang, L., and Xu, G. *Nanoscale*, 2013, 5 (8), 3172–3181.
[34] Murphy, C.J., Thompson, L.B., Chernak, D.J., Yang, J.A., Sivapalan, S.T., Boulos, S.P., Huang, J., Alkilany, A.M., and Sisco, P.N. *Curr. Opin. Colloid Interface Sci.*, 2011, 16 (2), 128–134.
[35] Xia, Y., Gilroy, K.D., Peng, H.C., and Xia, X. *Angew. Chemie - Int. Ed.*, 2017, 56 (1), 60–95.
[36] COMSOL multiphysics, *https://www.comsol.com/*.
[37] Gao, L., Lemarchand, F., and Lequime, M. *Thin Solid Films*, 2011, 520 (1), 501–509.
[38] Mukai, T., Azuma, C., Niibe, M., Yoshitani, Y., Kawakami, R., Nakano, Y., and Araki, Y. *Vacuum*, 2018, 152, 265–271.
[39] Kischkat, J., Peters, S., Gruska, B., Semtsiv, M., Chashnikova, M., Klinkmüller, M., Fedosenko, O., Machulik, S., Aleksandrova, A., Monastyrskyi, G., Flores, Y., and Ted Masselink, W. *Appl. Opt.*, 2012, 51 (28), 6789.
[40] Rago, R., Gorgerino, F., and Giordano, F. *Absorption and Scattering of Light by Small Particles*, Wiley-VCH Verlag GmbH, Weinheim, Germany.
[41] Mätzler, C. *Techinical Rep.*, 2002, Research report in University of Bern 2002-08.
[42] Laven, P., http://www.philiplaven.com/mieplot.htm.
[43] Link, S., and El-sayed, M.A. *Int. Rev. Phys. Chem.*, 2000, 19 (3), 409–453.
[44] Link, S., and El-sayed, M.A. 2000, 409–453.
[45] Du, L., Furube, A., Hara, K., Katoh, R., and Tachiya, M. *J. Photochem. Photobiol. C Photochem. Rev.*, 2013, 15 (1), 21–30.
[46] Bian, Z., Tachikawa, T., Zhang, P., Fujitsuka, M., and Majima, T. *J. Am. Chem. Soc.*, 2014, 136 (1), 458–465.